

# 博士論文（要約）

論文題目 A comprehensive understanding of  
modulators regulating tau aggregation  
(Tau タンパク質の凝集に関する因子の包括的理解)

氏名 櫻井 靖之

The microtubule associated protein tau is implicated in a broad range of neurodegenerative diseases collectively known as tauopathies, characterized by the accumulation of hyperphosphorylated and ubiquitinated insoluble aggregates of tau. To date, numerous studies have aimed to identify cellular pathways regulating the aggregation of tau. However, while several genetic screens utilizing *Drosophila* models of tau have been performed, no genome-wide screens using mammalian cells for modulators of tau aggregation have been reported. This is caused in part because no simple cell culture models of tau aggregation were available, since tau is a highly soluble, natively disordered protein, and overexpression alone does not induce aggregation of tau, as is the case for the poly-glutamine repeat expansion proteins. Recently, Sanders *et al.* reported a tau aggregation model cell line based on the microtubule binding repeat domain of tau (tau RD) that indefinitely propagates aggregates even after cell division (*Neuron*, 2014). Therefore, we performed a genome-wide siRNA screen for modulators of tau RD aggregation through utilizing this cell culture model.

We first independently reproduced the tau RD aggregation-propagating model cell line. HEK293A cells stably expressing tau RD fused to Venus was established (Fig. 1A). To increase the aggregation of tau RD, we introduced the P301L mutation, which is a causative mutation of frontotemporal dementia and is known to increase the aggregation propensity of tau. We next generated recombinant tau RD fibrils *in vitro* through incubation of purified tau RD with heparin (Fig. 1B). These recombinant tau RD fibrils were transduced into HEK293A cells stably expressing tau RD P301L-Venus through lipofection to induce aggregation of tau RD. Fibril-transduced cells containing tau RD aggregates were sparsely diluted, and monoclonal cell lines stably propagating tau RD aggregates, hereafter referred to as aggregate-positive cells, were obtained (Fig. 1C).

We used these aggregate-positive cells to perform high-content genome-wide siRNA screening based on quantification of the total intensity of cytoplasmic tau RD aggregates (Fig. 2A). For the 1<sup>st</sup> screening, we used a genome-wide siRNA library targeting approximately 18,000 genes, with 4 pooled siRNA constructs per gene, and selected 283 genes as significantly enhancing tau RD aggregation when knocked down (Fig. 2B). Representative images from the 1<sup>st</sup> screening are shown in Fig. 2C. To reduce off-target effects, from the 2<sup>nd</sup> screening, we used two different cell types and chemically modified siRNAs (Fig 2D). For the 2<sup>nd</sup> screening, we validated results of the 1<sup>st</sup> screening using HEK293A and U2OS tau RD aggregate-positive cell lines, again with 4 pooled siRNA constructs. Genes that were positive in both cell lines were taken as hits. Among these hit genes, we reasoned that some genes

would affect general protein degradation. To eliminate such genes, we performed a counter screen using HEK293A and U2OS cells stably expressing ZsGreen-mODC, a well-characterized proteasome model substrate consisting of the fluorescent protein ZsGreen fused to a mouse ornithine decarboxylase degron. Genes that caused accumulation of ZsGreen-mODC when knocked down likely affected proteasome activity, and were therefore removed from 2<sup>nd</sup> screening hits, resulting in 35 aggregation suppressor candidate genes. Finally, to further remove off-target effects, each of the 4 pooled siRNAs were tested individually in both HEK293A and U2OS tau RD aggregate-positive cell lines for the 3<sup>rd</sup> screening. Genes for which more than 3 of 4 individual siRNAs tested enhanced tau aggregation in either HEK293A or U2OS cells were chosen, resulting in 14 candidate aggregation suppressor genes.

Among these 14 genes, three genes were positive for 4 of 4 siRNA constructs tested in both cell lines (Fig. 2E). Of these, two were components of the SUMO modification (SUMOylation) pathway: SUMO2, and SAE1, a subunit of the SUMO activating E1 enzyme heterodimer. We therefore decided to investigate the role of SUMOylation on the aggregation of tau RD. Human cells express three isoforms of SUMO, of which SUMO2 and SUMO3 are nearly identical and often regarded as one protein, SUMO2/3, while SUMO1 is only about 50% identical to SUMO2/3. Therefore, we first tested the specificity of SUMO1 and SUMO2/3 modification through using 4 siRNA constructs against SUMO1, SUMO2, and SUMO3. We confirmed that only SUMO2 knockdown caused accumulation of tau RD aggregates in both HEK293A and U2OS cells. We further validated SUMO1 versus SUMO2/3 knockdown specificity on tau RD aggregation by flow cytometry following digitonin treatment to remove soluble tau RD, and confirmed that while knockdown of SUMO2/3 resulted in about a three-fold increase compared to non-targeting control siRNA, knockdown of SUMO1 had almost no effect on tau RD aggregates (Fig. 3A).

To facilitate immunoprecipitation (IP) of tau RD, we next established a HEK293T cell line stably expressing tau RD P301L-Flag-Halo (Fig. 1A). Using an aggregate-positive form of this cell line, SUMO1 and SUMO2/3 were knocked down, and the ubiquitination of tau RD-Flag-Halo was analyzed by Flag-IP followed by blotting for tau RD and K48-linked ubiquitin (Fig. 3B). This revealed that knockdown of SUMO1 and SUMO2/3 both increased the ubiquitination levels of soluble tau RD, with SUMO2/3 having a larger effect. In contrast, both SUMO1 and SUMO2/3 knockdown did not significantly affect the ubiquitination of insoluble tau RD.

We next investigated if tau RD was directly SUMOylated by overexpressing Myc-tagged SUMO1 or SUMO2 in a HEK293T tau RD aggregate-positive cell line, followed by Flag-IP of tau RD. Immunoblot analysis of immunoprecipitated tau RD from total cell lysate revealed additional higher molecular weight bands above that expected for tau RD (Fig. 4A). Comparison with immunoblots to detect SUMO and K48-linked ubiquitin revealed these bands to be due to both ubiquitination and SUMOylation of tau RD. Consistent with the effect of SUMO1 and SUMO2/3 knockdown increasing the ubiquitination of tau RD, we found that when UBE2I was overexpressed, there was a decrease in ubiquitination of tau RD. We then performed the same experiment using a HEK293T tau RD aggregate-negative cell line, and found that tau RD was also SUMOylated, and to a higher extent than in the aggregate-positive cell line (Fig. 4B).

Next, since the majority of tau RD expressed in aggregate-negative cell lines are soluble, we reasoned that SUMOylation may target soluble tau RD. We tested this through IP of tau RD from both the 0.2% Triton X-100 soluble and insoluble fractions of a tau RD aggregate-positive cell line. We found that soluble tau RD was mostly SUMOylated, while insoluble tau RD was mainly ubiquitinated (Fig. 5A and 5B).

Taken together, our results suggest a mechanism where SUMOylation competes with ubiquitination to prevent the aggregation of tau RD. While we do not currently have sufficient data to present a more detailed model, past studies have shown that SUMOylation can increase the solubility and inhibit the aggregation of misfolded proteins. Furthermore, SUMOylation has been shown to compete with the same lysine residue with ubiquitination, for example for I $\kappa$ B- $\alpha$ . Therefore, we propose a working hypothesis in which SUMO2 modification of tau RD maintains tau RD in a soluble state, thus inhibiting its aggregation and ubiquitination (5年以内に出版予定).

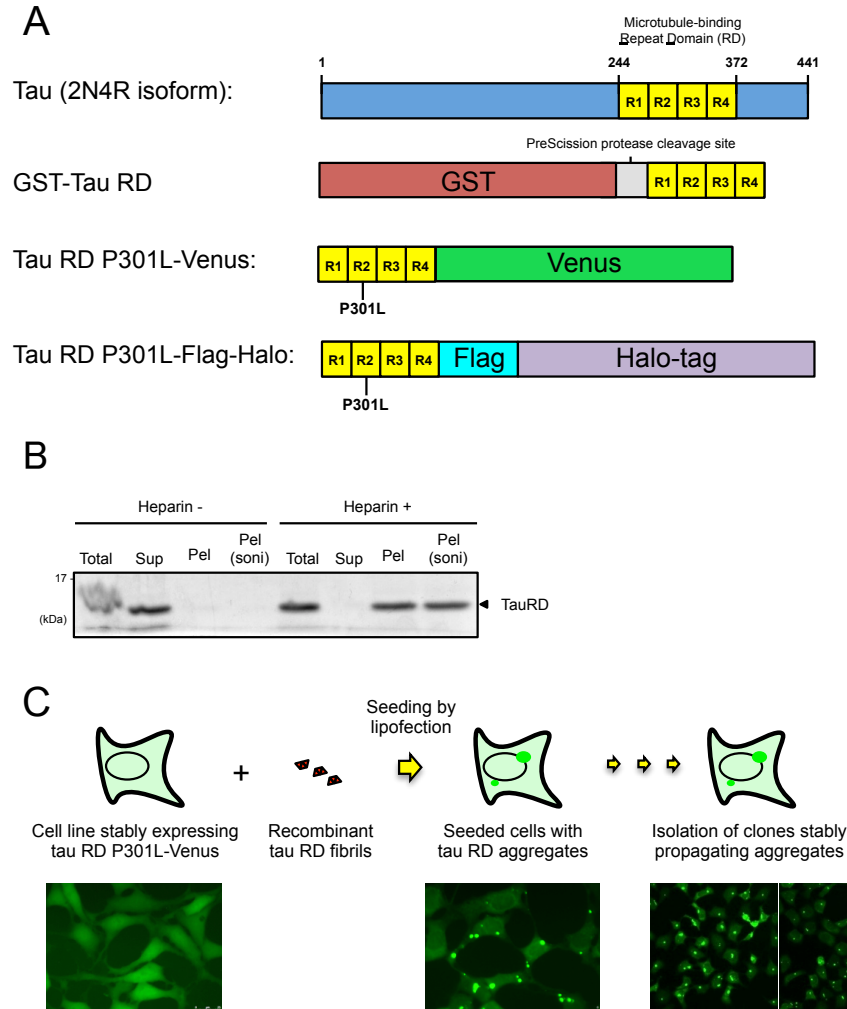
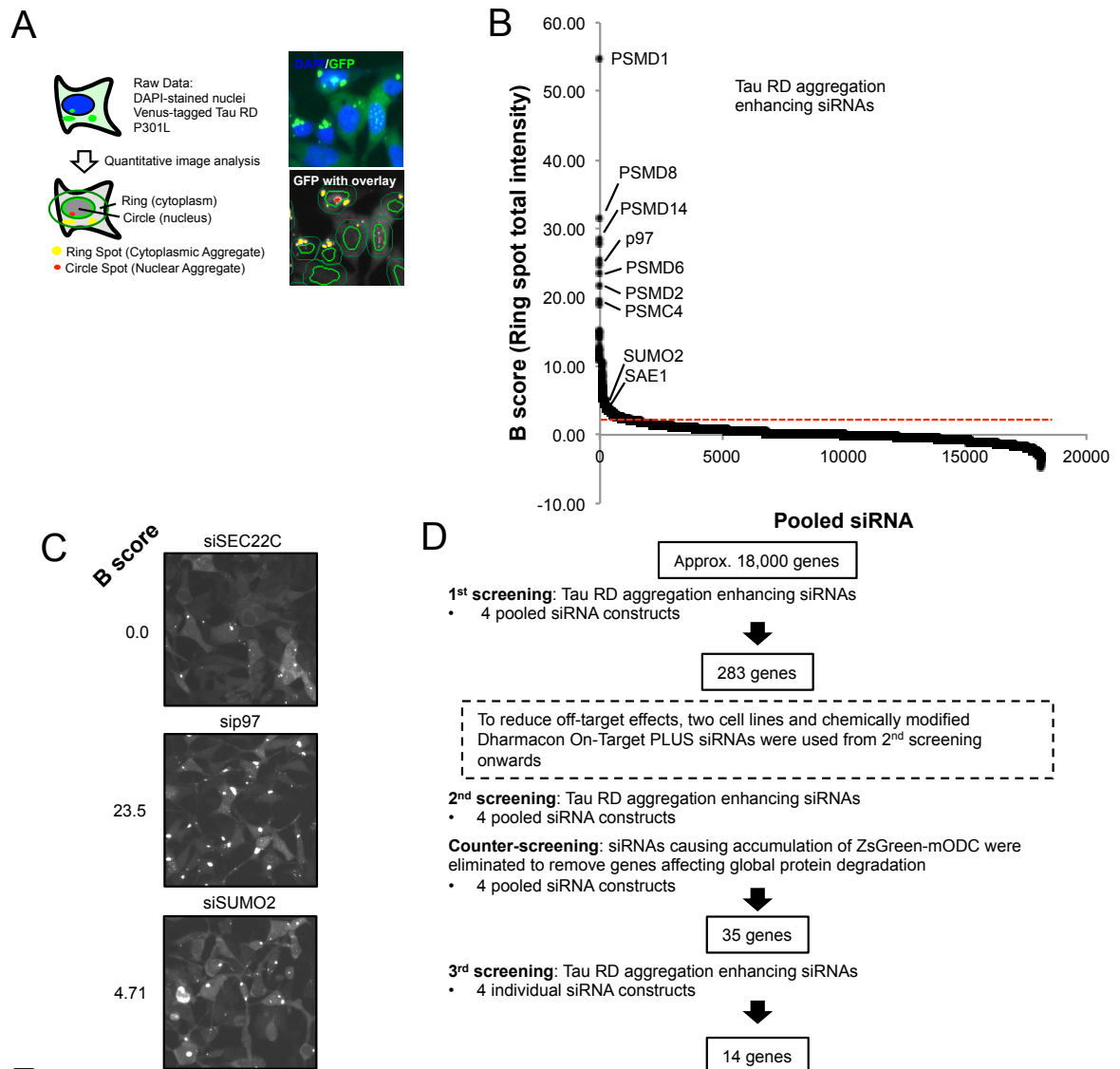


**Figure 1. Establishment of tau RD aggregate positive cell lines.** **A.** Schematic of constructs used in this study. The microtubule binding repeat domain (RD) from the 2N4R isoform of full-length tau was fused with an N-terminal GST-tag for recombinant tau RD production, and a C-terminal Venus or Flag-Halo-tag for cell culture experiments. To increase aggregation propensity, the P301L FTLD-17 mutation was introduced for all cell culture experiments. **B.** Ultracentrifugation analysis of recombinant tau RD fibrils obtained through incubation with heparin. After incubation with heparin, samples were centrifuged at 100,000 x *g* for 1 h, and divided into Total (before ultracentrifugation), soluble (Sup) and insoluble (Pel) fractions. The insoluble fraction was further sonicated (soni) to generate tau RD fibril seeds for transduction into cell cultures. **C.** Scheme for the establishment of cell lines stably propagating tau RD aggregates. A cell line stably expressing tau RD P301L-Venus was seeded with recombinant tau RD fibrils via lipofection. These seeded cells were then isolated and cloned into monoclonal cell lines stably propagating tau RD aggregates.



Gene name	Function	1st screening			2nd screening		3rd screening	
		B score (cutoff at 3.66)	z* score (cutoff at 4.3)	z* score (cutoff at 1.6)	293A	U2OS	293A	U2OS
SAE1	SUMO1 activating enzyme subunit 1	SUMO activating E1	4.20	13.48	35.11	4	4	
SUMO2	Small ubiquitin-like modifier 2	Post-translational modification	4.71	9.74	16.40	4	4	
TAF1	TATA-Box binding protein associated factor 1	Transcriptional regulation	8.71	51.22	70.05	4	4	
KPNB1	Importin Beta-1 subunit	Nuclear import	10.00	42.09	84.45	3	4	
MORC2	MORC family CW-type zinc finger 2	Transcriptional regulation	11.01	34.10	17.89	3	4	
BRD4	Bromodomain containing 4	Chromatin remodeling	4.32	21.64	112.06	3	4	
CBFA2T3	CBFA2/RUNX1 Translocation Partner 3	Transcriptional regulation	4.86	24.01	45.98	3	3	
CYLD	CYLD Lysine 63 Deubiquitinase	Deubiquitinase	6.32	16.71	26.03	3	3	
RGPD2	RANBP2-Like and GRIP domain containing 2	RNA transport	10.69	7.76	20.40	3	3	
FAM208A	FAM208A	Transcriptional regulation	14.95	36.07	18.16	4	2	
PABPC1	Poly-(A) binding protein cytoplasmic 1	mRNA binding	3.95	5.32	26.34	4	2	
ZFX	Zinc Finger Protein, X-linked	Transcriptional regulation	11.01	13.62	22.40	3	1	
HNRNPA2B1	Heterogenous Nuclear Ribonucleoprotein A2/B1	Splicing	6.04	13.83	29.31	3	1	
KIAA1551	KIAA1551	Unknown	8.30	18.58	18.75	4	1	

**Figure 2. Genome-wide siRNA screening identifies 14 aggregation enhancing siRNAs.** **A.** Schematic of high content image analysis. A region of set width (ring) around DAPI-stained nuclei (circle) was defined, and GFP spots within the ring were detected to quantify cytoplasmic tau RD aggregates. **B.** B scores of all samples in the 1<sup>st</sup> genome-wide siRNA screen based on cytoplasmic aggregate total fluorescence intensity. The cutoff value for siRNAs enhancing tau RD aggregation is indicated as a dashed red line. **C.** Representative images from the 1<sup>st</sup> screen. The cutoff value was decided based on inspection of such images as the value at which a clear difference between siRNAs with no effect (B score close to 0) and potential hit genes were visible. **D.** Overview of the siRNA screening protocol. 14 final candidate genes were obtained from approximately 18,000 siRNAs. **E.** Table of the 14 final candidate genes and an overview of their scores during the screening process.

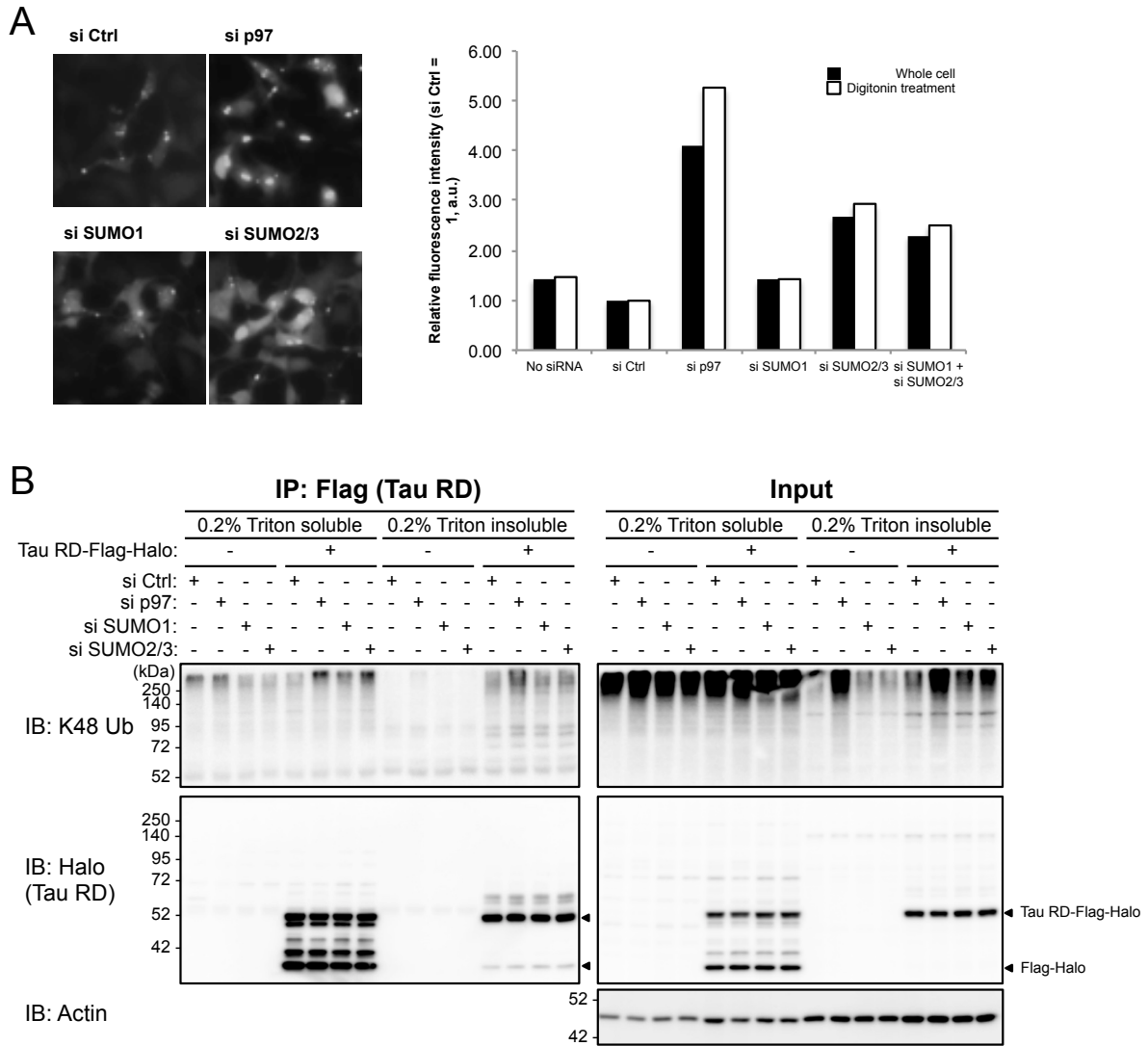
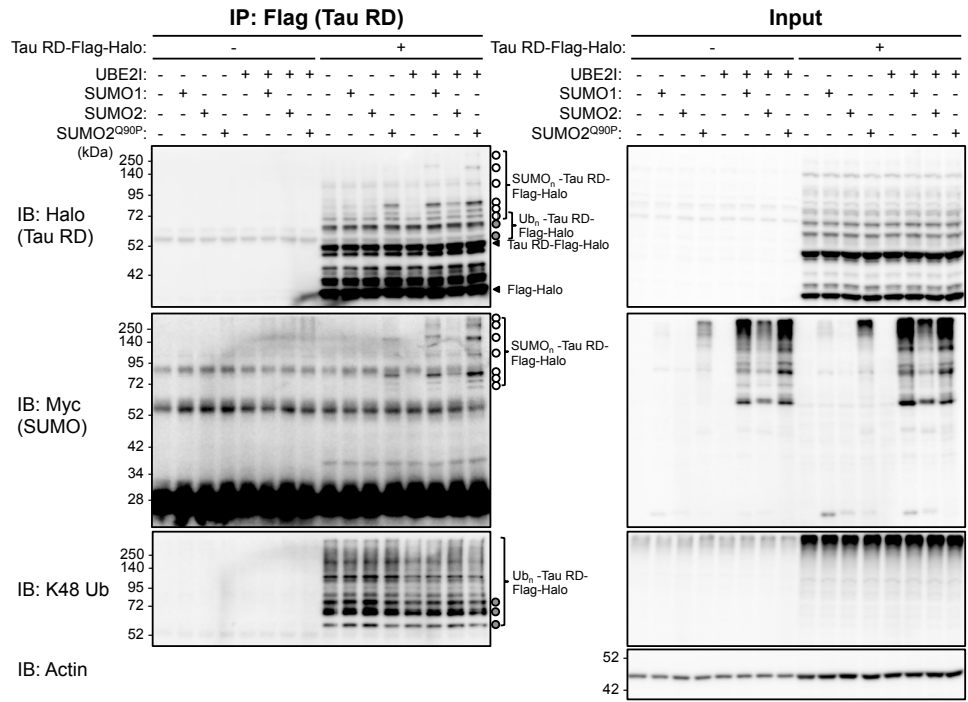


**Figure 3. Knockdown of SUMO2/3, but not SUMO1, affects tau aggregation and ubiquitination. A.** HEK293A tau RD P301L-Venus clone No. 2-2<sup>+</sup> cells were treated with the indicated siRNAs for 96 h, photographed, and then analyzed by flow cytometry through measuring Venus fluorescence intensity with and without digitonin treatment. Values are expressed as relative values with control siRNA (siCtrl) treatment set to 1. **B.** Effect of SUMO knockdown on the ubiquitination of tau RD. HEK293T tau RD P301L-Flag-Halo cells with tau RD aggregates (clone No. 2<sup>+</sup>) was treated with the indicated siRNAs, and tau RD was immunoprecipitated by Flag-IP from 0.2 % Triton X-100 soluble and insoluble fractions, and analyzed by immunoblot with the indicated antibodies.

### A IP from tau RD aggregate-positive cell line



### B IP from tau RD aggregate-negative cell line

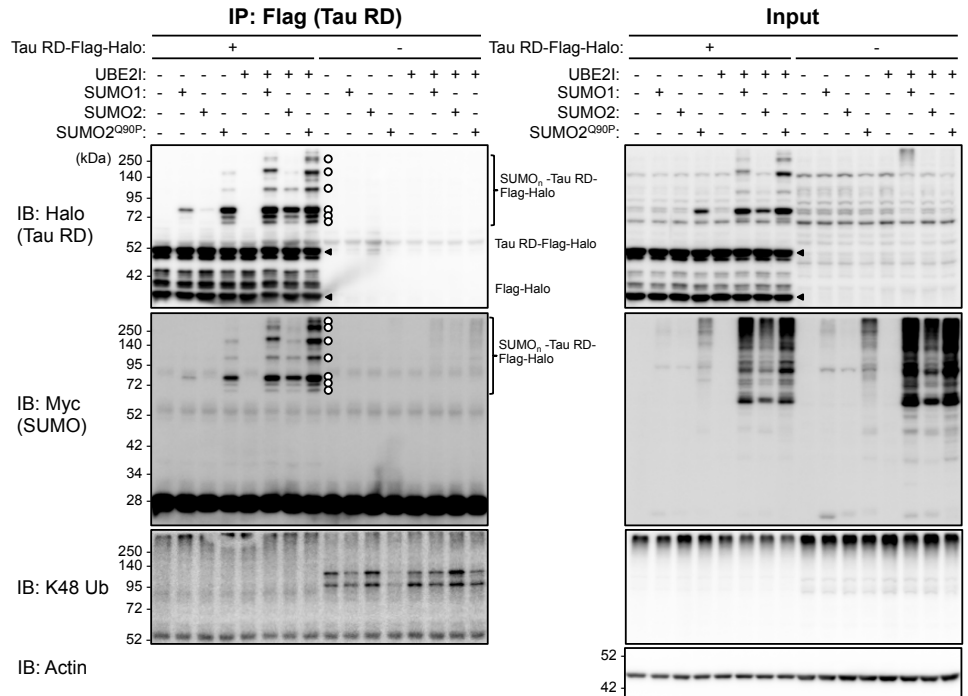
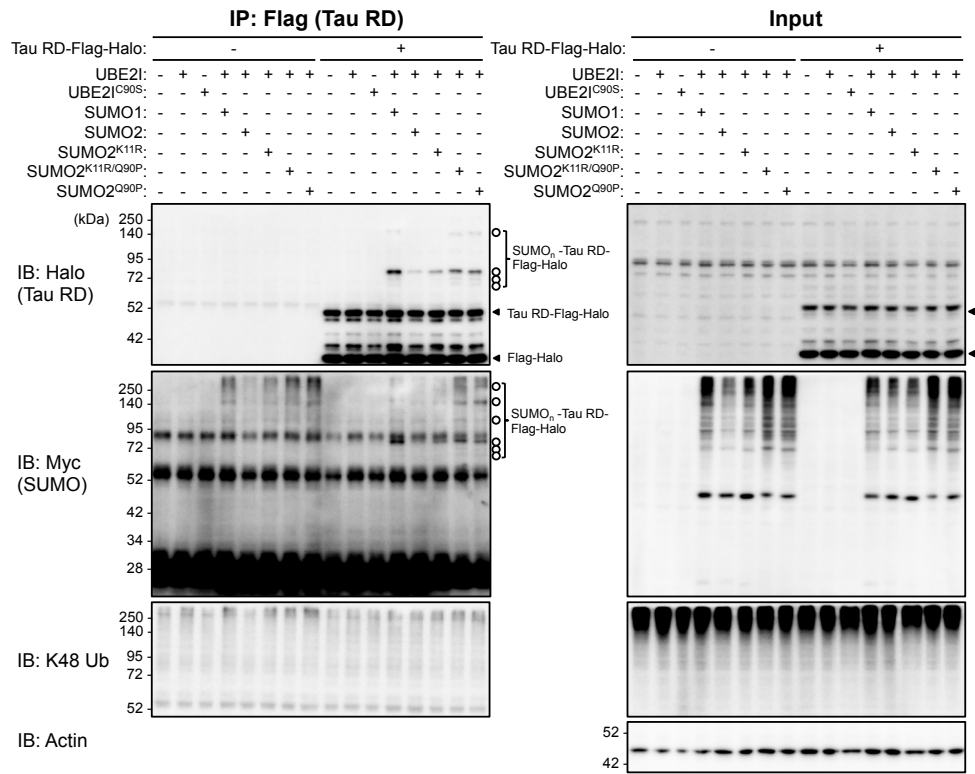


**Figure 4. Tau RD is directly SUMOylated in both aggregate-positive and aggregate-negative cells A.** Detection of tau RD SUMOylation by SUMO overexpression and immunoprecipitation of tau RD. HEK293T tau RD P301L-Flag-Halo cells with tau RD aggregates (clone No. 3\*) was transfected with the SUMO E2 ligase UBE21 and Myc-tagged SUMO1, SUMO2, or SUMO2<sup>Q90P</sup> (resistant to cleavage by SENP SUMO peptidases) as indicated, then tau RD was immunoprecipitated by Flag-IP from the 0.1% SDS soluble fraction. Bands due to SUMOylated and ubiquitinated tau RD are indicated as open and filled circles, respectively, based on comparison of the anti-Halo (tau RD) blots with the anti-Myc (SUMO) and anti-K48 ubiquitin blots. **B.** As in A, except that HEK293T tau RD P301L-Flag-Halo cells *without* tau RD aggregates (clone No. 2\*) was used instead.

**A** IP from 0.2% Triton X-100 soluble fraction



**B** IP from 0.2% Triton X-100 insoluble fraction

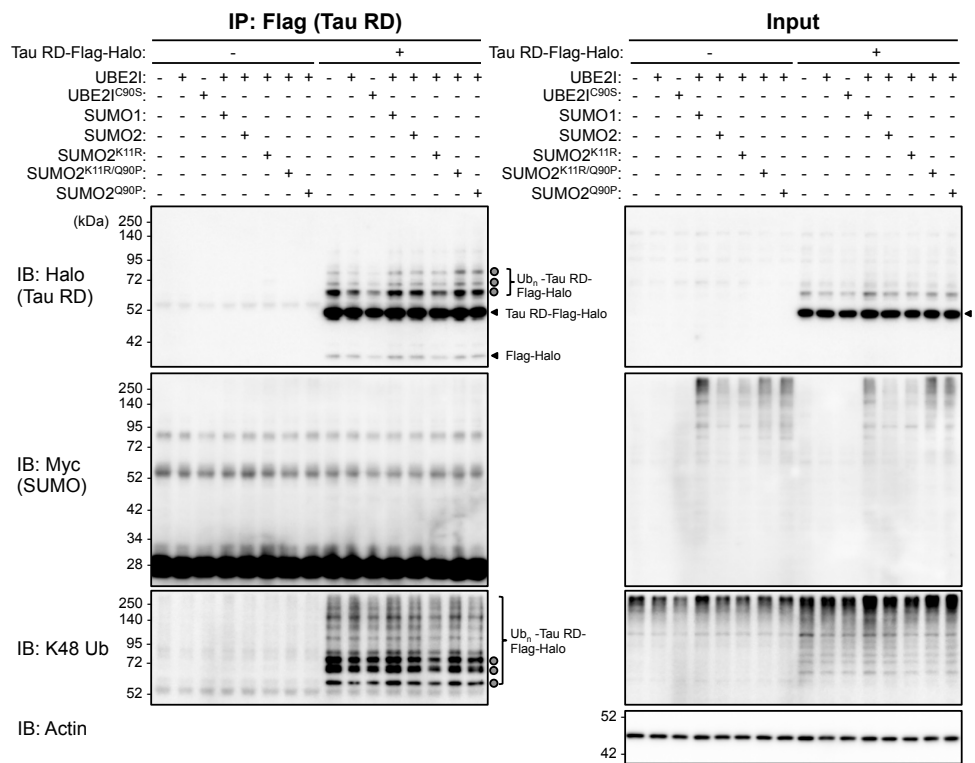


**Figure 5. Soluble tau RD is SUMOylated, while insoluble tau RD is ubiquitinated** **A.** Detection of tau RD SUMOylation by SUMO overexpression and immunoprecipitation of tau RD. HEK293T tau RD P301L-Flag-Halo cells with tau RD aggregates (clone No. 3\*) was transfected as indicated, and tau RD was immunoprecipitated from the 0.2 % Triton X-100 soluble fraction. Bands due to SUMOylated and ubiquitinated tau RD are indicated as open and filled circles, respectively, based on comparison of the anti-Halo (tau RD) blots with the anti-Myc (SUMO) and anti-K48 ubiquitin blots. **B.** As in A, but Flag-IP from the 0.2 % Triton X-100 insoluble fraction.